Earthquakes in Northwest Louisiana and the Texas–Louisiana Border Possibly Induced by Energy Resource Activities within the Haynesville Shale Play

by Jacob I. Walter, Peter J. Dotray, Cliff Frohlich, and Julia F. W. Gale

ABSTRACT

We utilize Transportable Array data to survey regional seismicity in east Texas and northwest Louisiana. Through analyst review and a waveform-matching technique, we identify 58 earthquakes occurring between April 2010 and July 2012. The earthquakes spatially cluster within two main zones, near Timpson, Texas, and within Bienville Parish, Louisiana; minor clusters occur in the Texas–Louisiana border region. Although the Timpson earthquakes have been studied previously, we identify many undetected earthquakes that occurred in 2010, about two years prior to the 17 May 2012 M_w 4.8 earthquake, which has been linked to wastewater injection. The Bienville Parish sequence, which consists of magnitude 0.5–1.9 earthquakes in mid- to late-2011, occurred about 10 km from wells that began injecting at relatively modest rates (~40, 000 barrels (bbl) per month) in late 2010 but within a few kilometers of production wells that were being hydraulically fractured around the same time period. An additional cluster of seismicity was observed, near Center, Texas, with some seismicity occurring in the months prior to the start of wastewater injection and the largest earthquake in that sequence occurring when injection exceeded 200, 000 bbl/month; this may be a case in which injection into a seismically active area promoted a larger earthquake. Finally, there was also seismicity observed near the Toledo Bend Reservoir in Louisiana. The evidence concerning some of the sequences indicates they might be associated with either hydraulic fracturing or recent increases in wastewater injection at wells within the unconventional Haynesville shale gas play. The results of this study highlight the need for more extensive seismic monitoring in the central and eastern regions of the United States of America.

Online Material: Figures of local versus U.S. Geological Survey magnitude for the events from 2010 to 2013 and distance correction for determining local magnitude, and tables of station and well information and the regional velocity model.

INTRODUCTION

In the last decade, incidents of increased seismicity throughout the central United States have been correlated with wastewater disposal to support oil and gas operations, commonly associated with unconventional hydrocarbon plays (e.g., Frohlich *et al.*, 2011, 2014; Horton, 2012; Keranen *et al.*, 2014; Rubinstein *et al.*, 2014). One such hydrocarbon play is the Haynesville shale play, which includes areas of east Texas and northwest Louisiana.

In many recent studies, whether seismicity is natural or associated with hydrocarbon activities is difficult to disentangle due to issues of seismic network coverage. This is coupled with the fact that the recent increase in earthquakes in the central United States has been occurring in a region that has been relatively sparsely instrumented. The monitoring coverage was considerably improved with the temporary (~2 yr) deployment of seismometers during the USArray Transportable Array (TA) experiment (see Data and Resources), which crossed the central United States in 2010–2012. This deployment presents a unique opportunity to understand intraplate seismicity and seismicity associated with unconventional hydrocarbon plays. We analyze the seismicity from April 2010 to July 2012 using this denser instrumentation (Ⓔ Table S1, available in the electronic supplement to this article).

Because the broad instrument spacing (~70 km) is not ideal for studying specific seismicity sequences, we utilize recently developed techniques to improve our seismicity catalogs. In addition to proximity issues, seismicity catalogs can be woefully incomplete for many reasons, including high station noise, earthquakes occurring closely spaced in time, or sparse network coverage. An effective way to identify possible "missing" events is the waveform matched-filter technique (e.g.,

doi: 10.1785/0220150193

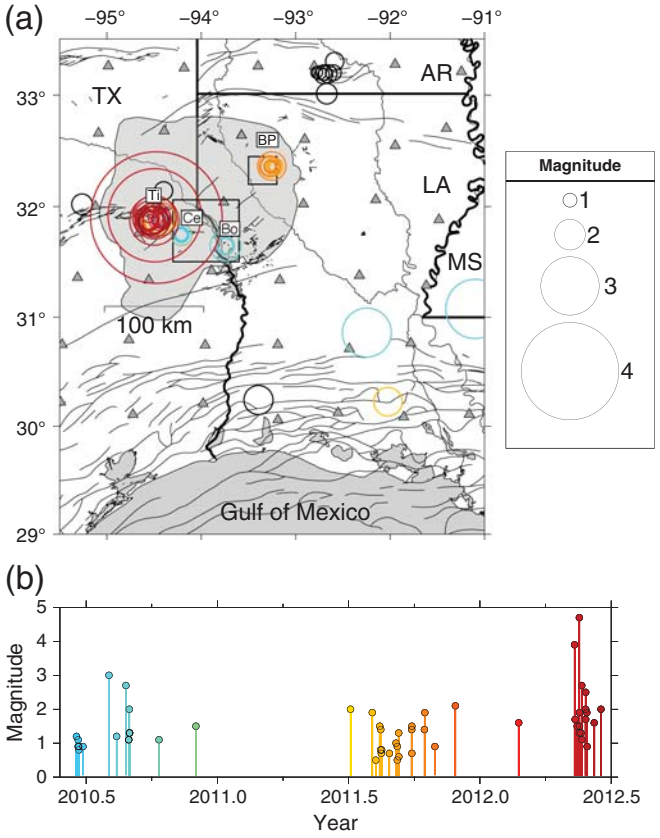

▲ **Figure 1.** (a) Map of study area, including earthquakes identified in this study. Color scheme progressing from blue to red indicates time of occurrence between early 2010 and mid-2012. Open black circles denote previous historical earthquakes identified by the Advanced National Seismic System (ANSS) Comprehensive Catalog in the years January 1980–February 2010 (see Data and Resources). Annotation on the map indicates locations of event clustering: Ti, Timpson; Ce, Center; Bo, border; and BP, Bienville Parish. Larger squares indicate areas shown in detail in Figures 4 and 5. States are identified with their abbreviations: TX, Texas; LA, Louisiana; (MS) Mississippi; and AR, Arkansas. Texas and Louisiana fault traces were obtained from the U.S. Geological Survey (USGS) Quaternary Faults and Folds Database (see Data and Resources) and from Ewing and Lopez (1991). The light gray shaded region in Texas and Louisiana is the extent of the Haynesville play from the U.S. Energy Information Administration (see Data and Resources). Triangles indicate the locations of USArray stations. (b) Local magnitude (M_L) over time period of this study for earthquakes shown in (a).

Shelly *et al.*, 2007; Walter *et al.*, 2015). Waveforms from earthquakes that are undetected but close spatially and that have similar focal mechanisms to cataloged events may transmit waveforms that appear similar upon inspection or are identified as similar by cross correlation. In this study, we use the matched-filter technique to identify earthquakes not detected by our initial automatic methods, allowing us to build a more comprehensive seismicity catalog with geographic emphasis near the Haynesville shale play (Fig. 1). Other studies have successfully used a waveform cross-correlation technique in the central United States with TA data (Kim, 2013; Skoumal *et al.*, 2014), and we use a comparable network-based cross correlation.

METHODS

Automatic Earthquake Detection

As in our previous study in the Williston Basin (Frohlich *et al.*, 2015), we first build a catalog utilizing standard passive seismological techniques for identifying earthquakes among continuous seismograms. We identify candidate phase arrivals utilizing an automatic short-term average/long-term average (STA/LTA) ratio filter with a threshold set based on our previous experience working with TA data. We catalog picks and determine trial locations and origin times using Antelope Seismic Database software. The phase arrivals and event associations are all analyst-reviewed and in all cases repicked manually. These phases are used to locate the events with the GENLOC earthquake location library (Pavlis *et al.*, 2004) as it is currently implemented in the *dbloc2* module of the Antelope seismic software using a 1D seismic velocity model for east Texas (Ⓔ Table S2), slightly modified from Frohlich *et al.* (2014). We utilize these events as templates for the next step in the analysis.

Waveform Matched-Filter Detection of "Missing" Earthquakes

We next identify additional events by applying the matched-filter technique. This technique utilizes waveforms of known events as a template to search for similar patterns in continuous recordings. It has been successfully applied to detect a myriad of unreported events that occurred at midocean ridges and transform faults (Shearer, 1994), as low-frequency earthquakes within the deep tectonic tremor signals (Shelly *et al.*, 2007), early aftershocks (Peng and Zhao, 2009), triggered earthquakes (Meng *et al.*, 2012), and foreshocks (Kato *et al.*, 2012; Walter *et al.*, 2015).

To run the matched-filter technique, we use the manually picked waveforms as initial templates. In order to focus on regional waveforms, we band-pass filter these data between 1 and 5 Hz, cut the waveforms 1 s before and 5 s after the phase arrival (*P* or *S*), and resample the data at 20 Hz. The filter and time cut are chosen to best represent the waveforms with high fidelity for the short distances (interstation TA distance ~70 km) and relatively short duration of the low-magnitude events for the resampled data. We utilize template events that have phase arrivals from at least four stations within the network. For each component and at each sample point through time, the matched-filter technique computes the normalized cross-correlation coefficient between the template and the continuous data to determine a normalized cross-correlation coefficient time series. Here "normalized" means the cross-correlation coefficient is between −1 and 1. The normalized coefficients for each component are then time-shifted back to the origin time and stacked. Detection occurs when the

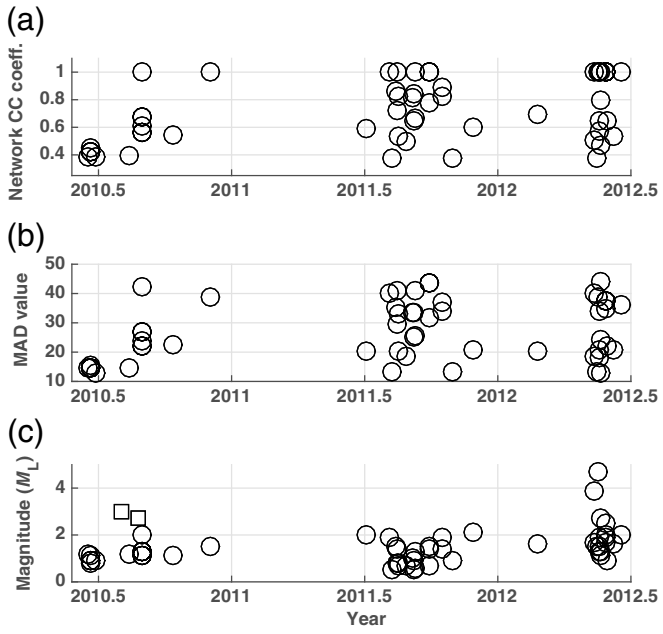

▲ **Figure 2.** Matched-filter results. (a) The network-averaged cross-correlation coefficient (CC coeff.), for which a value of 1 indicates a self-detection of a template event. (b) Median absolute deviation (MAD) of the stacked cross correlation. (c) M_L of both template and matched-filter events. The square symbols indicate earthquakes in southern Louisiana that had no matching templates and do not appear in (a) or (b).

stack initially exceeds nine times the median absolute deviation (MAD), a threshold similar to that employed by other studies utilizing a network-based matched-filter technique (e.g., Meng *et al.*, 2013). We examined these initial detections and, after careful analyst scrutiny, chose a higher threshold of 12 times the MAD (Fig. 2), which was sufficient to ensure that visible body waves were present on seismograms for at least a few stations for the newly detected events. Note that this is a more conservative approach, reducing the possibility of false detections.

Once matches are identified, we further improve the relative locations of the newly identified events rather than assuming they have the same spatial origin as the template event. We cross-correlate individual phases of each newly detected event relative to the master template event to obtain differential timing of arrival phases at each component and to include phase shifts when this cross-correlation coefficient exceeds 0.4. These relative phase shifts, if they are present, are used in *hypoDD* (Waldhauser and Ellsworth, 2000) to obtain a relative location for the newly detected event with respect to the template event. Sometimes no phase shift is detectable; and, in these cases, the assigned location is plotted at the same epicenter as the template event.

Magnitude Determination

The default magnitude determination routine within Antelope (*dbevproc*) computes the Richter magnitude, otherwise known as the local magnitude M_L. M_L is calculated at each station with the equation

$$M_L = \log_{10} A - \log_{10} A_0(\Delta) + c, \quad (1)$$

in which $\log_{10} A$ is the base-10 logarithm of peak amplitude A (in millimeters) on a Wood–Anderson seismometer, station Δ (in kilometers) is the source–station distance, and C is a station correction term. The $\log_{10} A_0$ (Δ) term is the amplitude–distance correction, which is a function of Δ and was originally empirically determined for southern California (Richter, 1935). This correction was originally fixed such that, on the Wood–Anderson seismometers that were once commonly used throughout southern California, the peak amplitude was 1 mm for an M_w 3.0 earthquake recorded at a source–station distance of 100 km. Richter (1958) provided a table of correction values for the $\log_{10} A_0$ term, and the Antelope program uses those values for calculating M_L. M_L is calculated for each individual station, and the event magnitude is the mean of those values.

Upon comparison of the event magnitudes initially calculated for earthquakes that were also reported by the Advanced National Seismic System (ANSS) Comprehensive Catalog (see Data and Resources), we found that our initial magnitudes were, on average, ~0.8 magnitude units higher (Ⓔ Fig. S1). As in other previous regional studies (e.g., Hutton and Boore, 1987; Kim, 1998; Kang *et al.*, 2000), we utilize equation (1) to determine a more reasonable value for the distance-correction term $\log_{10} A_0$ for our study region by setting M_L equal to the ANSS magnitude and plotting $\log_{10} A_0$ as a function of distance to each station. Then, using least-squares to fit our data for east Texas, we find the following distance-correction term for east Texas when computing M_L: $-\log_{10} A_0 = 1.91(\log_{10} \Delta) - 1.55$ (Ⓔ Fig. S2). When we compare our correction with those determined for southern California (Richter, 1935; Hutton and Boore, 1987) over epicentral distances of 50–400 km, our correction is ~0.8 magnitude units higher, which is the cause of the discrepancy between our initial magnitude calculations and those provided by the ANSS Comprehensive Catalog. Thus, to obtain a magnitude for our study region, we utilize the following equation:

$$M_L = \log_{10} A - 1.91 \log_{10}(\Delta) + 1.55. \quad (2)$$

We use equation (2) to calculate magnitudes for the template events. Equation (2) allows us to calculate magnitudes that are, on average, equal to the ANSS-published magnitude ±0.1 magnitude units. For each component and each event detected by the matched-filter technique, instead of equation (2), we estimate the magnitude of the new event by calculating the ratio between the peak amplitude of the newly detected event and the original template event amplitude. The median value of all the ratios is used to calculate the new event magnitude, assuming a logarithmic scaling between event amplitude and magnitude (Peng and Zhao, 2009; Walter

Table 1
Haynesville Area Events (April 2010–July 2012)

Day (yyyy/mm/dd)	Time (hh:mm:ss.ss)	Latitude (°)	Longitude (°)	Depth (km)	Magnitude	CC	MAD	Cluster*
2010/04/22	03:00:40.38	31.884	−94.436	0.3	0.8	0.45	15.8	Ti
2010/06/17	20:05:26.74	31.884	−94.435	0.3	1.2	0.38	14.7	Ti
2010/06/20	06:17:16.05	31.744	−94.210	5.1	1.1	0.43	14.6	Ce
2010/06/20	09:23::27.31	31.745	−94.209	5.1	0.9	0.45	15.5	Ce
2010/06/21	04:42:29.00	31.744	−94.209	5.1	0.9	0.42	14.6	Ce
2010/06/21	07:36:36.95	31.744	−94.210	5.1	0.8	0.42	14.7	Ce
2010/06/27	03:08:07.10	31.744	−94.209	5.1	0.9	0.39	12.8	Ce
2010/08/02	04:34:30.60	31.074	−91.100	37.0	3.0	—	—	SM
2010/08/12	19:00:21.34	31.884	−94.436	0.3	1.2	0.39	14.8	Ti
2010/08/25	19:35:01.58	30.860	−92.247	34.4	2.7	—	—	SL
2010/08/29	19:58:25.72	31.645	−93.745	0.5	1.1	0.57	21.9	Bo
2010/08/29	19:59:54.00	31.645	−93.745	0.5	1.1	0.57	21.9	Bo
2010/08/30	14:05:31.98	31.644	−93.744	0.5	2.0	1.00	42.2	Bo
2010/08/30	15:07:04.47	31.645	−93.745	0.5	1.3	0.61	23.9	Bo
2010/08/30	21:38:40.00	31.644	−93.745	0.5	1.3	0.68	27.1	Bo
2010/08/30	21:56:01.88	31.645	−93.744	0.5	1.3	0.68	27.1	Bo
2010/10/10	21:11:14.04	31.885	−94.436	0.3	1.1	0.54	22.7	Ti
2010/12/01	04:05:46.81	31.744	−94.210	5.1	1.5	1.00	39.0	Ce
2011/07/04	02:36:35.85	31.901	−94.438	2.0	2.0	0.60	20.4	Ti
2011/08/03	11:08:50.68	30.227	−92.023	62.1	1.9	1.00	40.2	SL
2011/08/08	09:18:11.48	32.361	−93.268	2.6	0.5	0.38	13.4	BP
2011/08/13	18:15:08.68	32.360	−93.268	2.8	1.5	0.86	35.2	BP
2011/08/14	21:53:37.10	32.360	−93.269	2.7	0.8	0.72	29.4	BP
2011/08/15	04:12:28.36	32.361	−93.268	2.8	1.4	1.00	41.2	BP
2011/08/16	00:56:31.74	32.361	−93.269	2.7	0.7	0.54	20.3	BP
2011/08/16	08:48:26.47	32.360	−93.268	2.7	0.8	0.82	33.2	BP
2011/08/27	03:53:54.75	32.361	−93.268	2.7	0.7	0.50	18.6	BP
2011/09/05	11:52:14.16	32.359	−93.227	5.0	1.0	0.82	33.7	BP
2011/09/07	03:24:45.06	32.360	−93.228	5.0	0.9	0.84	33.5	BP
2011/09/07	06:11:23.41	32.359	−93.227	5.1	0.5	0.65	25.0	BP
2011/09/09	04:48:34.28	32.359	−93.228	4.9	1.3	1.00	41.0	BP
2011/09/09	09:34:02.07	32.359	−93.228	5.1	0.6	0.66	25.8	BP
2011/09/27	06:39:43.13	32.361	−93.268	2.8	1.4	0.77	31.8	BP
2011/09/27	09:17:35.28	32.365	−93.273	7.4	1.5	1.00	43.5	BP
2011/09/27	09:25:17.87	32.364	−93.275	7.4	0.7	1.00	43.5	BP
2011/10/14	22:31:22.78	32.361	−93.268	2.8	1.4	0.82	34.1	BP
2011/10/15	10:55:41.90	32.365	−93.253	1.3	1.9	0.89	36.9	BP
2011/10/29	09:19:28.53	32.360	−93.268	2.8	0.9	0.37	13.4	BP
2011/11/26	21:22:13.06	31.887	−94.434	0.3	2.1	0.60	20.8	Ti
2012/02/23	01:21:03.23	31.886	−94.437	0.3	1.6	0.69	20.4	Ti
2012/05/10	15:15:40.49	31.920	−94.493	7.6	3.9	1.00	40.3	Ti
2012/05/11	08:35:44.53	31.891	−94.573	35.5	1.7	0.50	18.7	Ti
2012/05/14	07:37:07.82	31.886	−94.581	37.6	1.5	0.38	13.4	Ti
2012/05/17	08:12:02.79	31.900	−94.476	3.5	4.7	1.00	38.8	Ti

CC, cross-correlation coefficient; MAD, median absolute deviation. Note two events were detected but not used for the matched-filter technique due to a limited number of stations with phase arrivals (no CC or MAD values reported in the table).
*Clusters: Ti, Timpson; Ce, Center; Bo, border; SL, southern Louisiana; SM, southern Mississippi; BP, Bienville Parish.
(Continued next page.)

Table 1 (continued)
Haynesville Area Events (April 2010–July 2012)

Day (yyyy/mm/dd)	Time (hh:mm:ss.ss)	Latitude (°)	Longitude (°)	Depth (km)	Magnitude	CC	MAD	Cluster*
2012/05/17	08:46:06.53	31.873	−94.557	30.9	1.3	0.57	18.0	Ti
2012/05/17	10:58:53.90	31.868	−94.553	31.3	1.9	1.00	33.8	Ti
2012/05/17	14:09:21.18	31.871	−94.557	31.1	1.5	0.65	20.7	Ti
2012/05/19	16:37:12.97	31.886	−94.437	0.3	1.3	0.47	13.0	Ti
2012/05/20	18:28:35.30	31.873	−94.498	26.9	2.7	1.00	44.0	Ti
2012/05/20	19:08:58.54	31.886	−94.437	0.3	1.1	0.80	24.3	Ti
2012/05/26	05:42:25.27	31.850	−94.518	30.2	1.7	1.00	37.6	Ti
2012/05/26	05:47:59.41	31.900	−94.493	8.1	2.0	1.00	37.6	Ti
2012/05/26	05:58:27.80	31.903	−94.499	8.6	2.5	1.00	37.6	Ti
2012/05/27	17:35:27.28	31.919	−94.556	7.7	1.9	1.00	34.8	Ti
2012/05/28	03:31:22.93	31.914	−94.555	7.5	0.9	0.65	22.0	Ti
2012/06/07	00:34:48.45	31.864	−94.501	27.5	1.6	0.54	21.0	Ti
2012/06/16	08:58:13.98	31.890	−94.517	21.5	2.0	1.00	36.3	Ti
2012/07/19	19:08:00.48	31.863	−94.500	27.4	2.0	0.69	28.5	Ti

CC, cross-correlation coefficient; MAD, median absolute deviation. Note two events were detected but not used for the matched-filter technique due to a limited number of stations with phase arrivals (no CC or MAD values reported in the table).
*Clusters: Ti, Timpson; Ce, Center; Bo, border; SL, southern Louisiana; SM, southern Mississippi; BP, Bienville Parish.

et al., 2015). Relative magnitude associations for cross-correlated data may be prone to errors for low cross-correlation coefficient results (e.g., Schaff and Richards, 2014). However, our data should be a reasonable approximation of the event magnitude because we have used a relatively conservative data-processing strategy: we select events using a relatively high MAD, we require that an analyst also visually identifies the detected event, and that the newly detected events have a relatively high cross-correlation value (median value of 0.59 for all newly detected events in Table 1).

RESULTS AND DISCUSSION

Seismicity

We identify 19 earthquakes using the STA/LTA method described in the Automatic Earthquake Detection section. When we used these as template events and applied the matched-filter technique, we identify a total of 58 earthquakes (Fig. 1 and Table 1). Most of the newly identified earthquakes have smaller magnitudes than the 19 template events (Fig. 2). The template events are easily identified because they have a cross-correlation coefficient equal to 1.0 in Figure 2a. Most of the earthquakes occur in clusters originating from five distinct foci.

Timpson Cluster

The most numerous cluster, with 25 earthquakes (Fig. 3a), occurred adjacent to the town of Timpson in east Texas and includes 13 events reported by Frohlich *et al.* (2014). Our study attempts to analyze seismicity in mid-2012 during the time period when the TA stations were being removed from east Texas; many of the stations detecting seismicity were located in Louisiana at this time. Thus, Frohlich *et al.* (2014) should be consulted for their analysis of the Timpson aftershock seismicity using a temporary network installation beginning 26 May 2012, nine days after the M_w 4.8 Timpson mainshock occurred. We identified four earthquakes (labeled "Ti" in Table 1) between the M_w 4.8 earthquake and the temporary network install, highlighting the usefulness of the matched-filter technique for early aftershock detection and

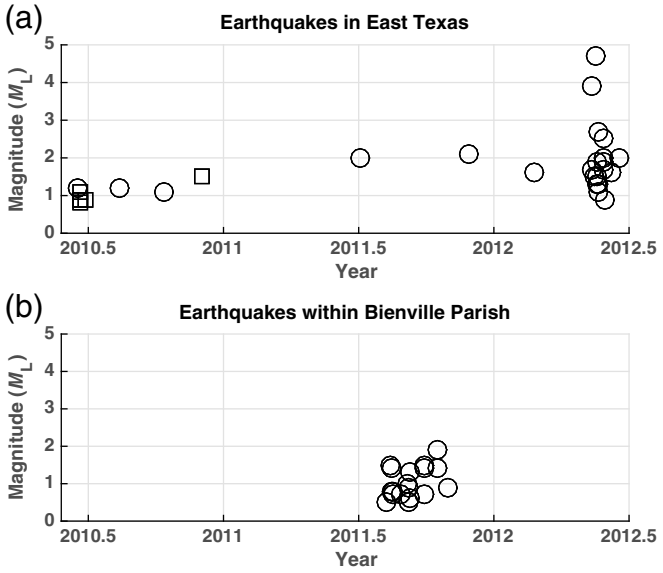

▲ **Figure 3.** Earthquakes within two distinct regions of (a) east Texas (circles, Timpson cluster; squares, Center cluster) and (b) Bienville Parish, Louisiana.

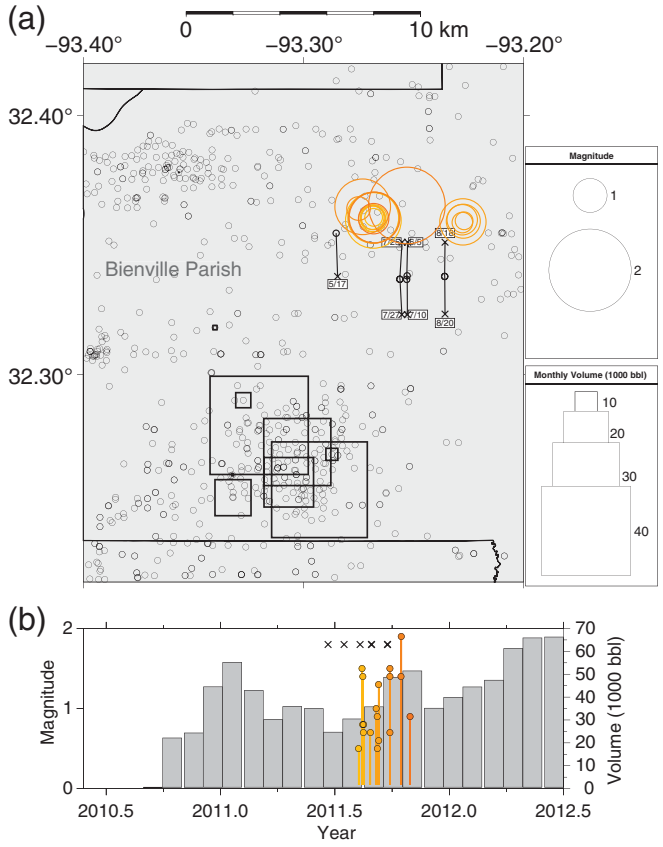

▲ **Figure 4.** Earthquakes and wastewater injection wells in the Bienville Parish, Louisiana. (a) Locations of Bienville Parish (BP) earthquakes (orange circles), injection wells with mean monthly injection volumes from 2010 through 2012 (black squares), and production wells (light gray circles). The mapped horizontal production wells are those completed May–August 2011 using hydraulic fracturing techniques (each bold black × indicates a bottom hole location, each bold black circle, is a surface hole location; and labeled dates indicate the completion dates of hydraulic fracturing, which occurs over 3–8 days at each well. True vertical depths are ∼11,500–12,000 ft at the bottom hole locations. See Ⓔ Table S4). Note that earthquakes are 10–12 km from injection wells and within a few kilometers of production wells that were hydraulically fractured near the origin times of the events. (b) Bienville Parish earthquake magnitudes are shown as a function of time and total monthly volumes for injection wells and hydraulically fractured horizontal well completion dates (black ×) are from (a). During the time period 2005–2010.5, no injection occurred, as reported to Louisiana Department of Natural Resources.

before network densification, when station coverage is otherwise too sparse to detect small aftershocks. In addition, among the Timpson events we identified are four earthquakes occurring in 2010, one in 2011, and seven in 2012 that were not identified by Frohlich *et al.* (2014), including two earthquakes occurring after the 10 May 2012 M_L 3.9 earthquake and prior to the 17 May 2012 M_w 4.8 earthquake. This confirms that sustained seismic activity occurred 1.5–2 yr prior to the 17 May 2012 M_w 4.8 earthquake, a finding consistent with Frohlich *et al.* (2014).

Bienville Cluster

The second-largest cluster identified in this study had 18 earthquakes and occurred in the northwestern portion of Louisiana, within the Bienville Parish and between the towns of Jamestown and Ringgold (Fig. 3b). These earthquakes (labeled "BP" in Table 1) all occurred in August, September, and October of 2011 and were not reported by other agencies. Of particular note is the number of smaller magnitude earthquakes without a preceding larger event. Clearly these events are not part of some aftershock sequence and are instead most consistent with classification as a seismic swarm. However, many of the stations adjacent to the Bienville Parish area were removed in January 2012, as the network was repositioned eastward. Thus, our ability to detect earthquakes after the end of 2011 was greatly diminished.

Center Cluster

A third cluster had six earthquakes, five occurring in June and one in December of 2010, about 25 km southeast of the Timpson cluster (Fig. 3). This is ∼6 km south of Center, Texas and several kilometers east of a location determined for an earthquake felt in Center in 1981 and recorded by a temporary local network (Pennington and Carlson, 1984; Frohlich and Davis, 2002). The six earthquakes in this Center cluster (labeled "Ce" in Table 1) appear to be separate from the Timpson cluster; because they were recorded mostly by the same stations, it is implausible the epicenters are grossly mislocated.

Border Cluster and Other Events

We also located earthquakes in other areas of Louisiana. A fourth cluster of six earthquakes (labeled "Bo" in Table 1) occurred over two days in August 2010, just east of the Louisiana–Texas border. Finally, we located two earthquakes in southern Louisiana and Mississippi in August 2010 and one earthquake in southern Louisiana in August 2011. Of the three, only one was identified by ANSS during 2 August 2010 (ANSS Comprehensive Catalog, see Data and Resources). Although the epicenters reported elsewhere in the article are accurate to ±2 km, the epicenters of the earthquakes in southern Louisiana and Mississippi may be inaccurate by 10 s of kilometers, because there was a paucity of seismic stations in southern Louisiana when they occurred (no TA stations were in Louisiana until early 2011).

Relation to Wastewater Injection and Hydraulic Fracturing

Timpson Cluster

Frohlich *et al.* (2014) link the spatial and temporal occurrence of earthquake activity near Timpson to wastewater injection into the Rodessa Formation there. Nearby injection into wells that were disposing of 100,000–200,000 bbl/month as early as 2006 was the possible cause of that seismicity (Frohlich *et al.*,

2014; McGarr, 2014). Fluid injection in one well occurs within 1 km of the tip of a mapped blind fault that was identified to have slipped during the May 2012 aftershock sequence. Our findings confirm that seismicity was occurring in the years prior to the 17 May 2012 earthquake (Frohlich *et al.*, 2014), because we are able to identify different events than those identified in that study for the years preceding the Timpson mainshock.

Bienville Cluster

For Bienville Parish, we compiled injection well volumes for Bienville Parish within the archives of the Louisiana Department of Natural Resources, utilizing a paid research service (Ⓔ Table S5). Between 2005 to present there were 51 injection wells within the Parish. We included only the 14 wells closest to the epicenters identified within the western portion of Bienville Parish, shown in Figure 4 (Ⓔ Table S3).

There was no reported wastewater injection in the Bienville Parish area from 2005 to late 2010 (Fig. 4). The seismicity we detect there occurred during peak monthly injection volumes around mid- to late-2011. Using a 1D seismic velocity model (Ⓔ Table S1) tuned to local geology in the Timpson area (Frohlich *et al.*, 2014), we find that injection at a few wells at 40, 000 bbl/month occurs within 10 km of the cluster of epicenters shown in Figure 4. We note that the horizontal error for epicenters is on the order of $\sim \pm 2$ km. Due to the 70 km station spacing, the earthquake focal depths are not reliable.

Closer to the cluster of seismicity (within a few kilometers) were a number of production wells that were being completed around the time of the seismicity (Fig. 4; Ⓔ Table S4). Based on our review of regulatory filings, they were being hydraulically fractured from May through August 2011. However, high-resolution reflection seismic data, which in some cases delineates buried faults or other geomechanical features (e.g., Hornbach *et al.*, 2015), are not publicly available in the area of interest.

The presence of seismicity during the months experiencing high wastewater injection rates (Fig. 4b), including the largest magnitude event during the highest monthly injection rate during calendar year 2011 suggests that earthquake activity could be coincident with relatively high injection rates. In mid-2012, injection rates were higher, though the TA stations were no longer present and thus our ability to detect seismicity in the area during 2012 was greatly diminished. The potential correlation between injection rate and the presence of seismicity would be an observation consistent with a recent study of the spatial correlation (~10 km) between earthquakes and high-rate injection wells across the central United States (Weingarten *et al.*, 2015). Although, as that study and other recent studies highlight (e.g., Hornbach *et al.*, 2015), the lack of pore pressure monitoring at depth makes it difficult to determine the factors that trigger the seismicity. The epicenters in Bienville Parish are actually closer to production wells than to the injection wells. Moreover, because of the absence of nearby seismic stations near Bienville Parish prior to 2010, it is possible that small swarms of natural origin had occurred here or in other parts of northern Louisiana previously but went undetected. Though hydraulic fracturing typically produces very small earthquakes ($\sim M_w$ 0 and below; Rubinstein and Mahani, 2015), there are recent studies that show hydraulic fracturing has caused earthquakes of moderate size ($\sim M_L$ 2–3) but generally not felt by humans except in a few cases (e.g., Friberg *et al.*, 2014; Skoumal *et al.*, 2015) and has even induced earthquakes up to M_L 4.4 (BC Oil and Gas Commission, 2014). In the case of the Bienville Parish, the hydraulically fractured wells also appear to be relatively deep compared with production wells in other shale plays (true vertical depths are ~11, 500–12, 000 ft). Because background lithospheric stresses are greater at depth, injection into critically stressed zones may preferentially induce earthquakes large enough to be detected by regional seismic networks. Regardless of the specific contributing factors, hydraulic fracturing appears to be the most likely cause of seismicity in the Bienville Parish, though natural fault slip could have also caused the seismicity.

Center and Border Clusters

Two other clusters of note include the Center cluster, located near the town of Center, Texas, and the border cluster, near the east side of Toledo Bend Reservoir in Louisiana (Fig. 5). These clusters are about 30 and 80 km, respectively, from the Timpson earthquakes. Both clusters are within 5 km of an active injection well (Fig. 5). The Center seismicity and injection occur adjacent to a mapped fault (Geomap Company, 2012). The seismicity is clearly present prior to injection at the adjacent well (Fig. 5b), but the largest magnitude event occurred on 1 December 2010 during a period of time when monthly wastewater injection exceeded 200, 000 bbl/month. If the larger event was induced by wastewater injection, then the observations suggest that injection in an area already experiencing seismicity may cause further events to occur. Alternatively, all events could be natural. The border cluster is adjacent to injection wells (within 5 km), though those wells inject at significantly reduced rates (~40, 000 bbl/month) compared with the injection well adjacent to Center.

There is also recent historical seismicity near the east Texas border with Louisiana. In 1964, there were a number of earthquakes over a three-month period along the Texas–Louisiana border during the time period when the Sam Rayburn Reservoir and the Toledo Bend Dam were under construction but before water impoundment (Henley, 1965; Stevenson and McCulloh, 2001; Frohlich and Davis, 2002). The area near Center also has experienced a number of earthquakes, including one M_w 3.0 in 1981 (Pennington and Carlson, 1984) and two earthquakes in the period since the TA was removed from the area, including an M_w 2.1 in 2013 and an M_w 3.1 in 2014 (Fig. 5). Although there are no injection wells within 5 km of the 2014 earthquake, there is an injection well within 4 km of the 3 February 2013 earthquake, and that injection well exceeded 400,000 bbl in the month of January 2013 (Texas Railroad Commission Public GIS Viewer, see Data and Resources), possibly triggering that event. Clearly there is a questionable

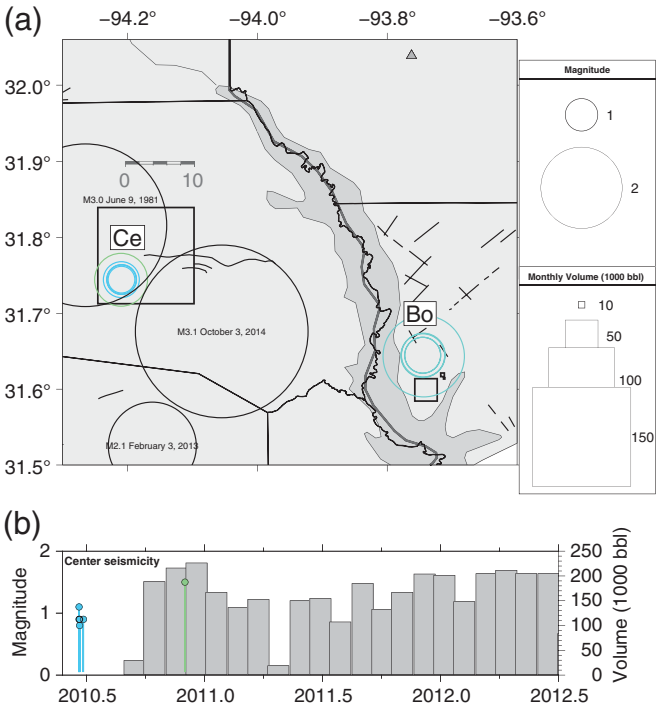

▲ **Figure 5.** Earthquakes and wastewater injection wells near the Center and border clusters. (a) Locations of Center and border earthquakes and injection wells with mean monthly injection volumes. Both clusters are 4–5 km from injection wells. Fault traces are from the USGS Quaternary Faults and Folds Database (see Data and Resources), and the fault trace near the Center cluster is from Geomap Company (2012). Other earthquake epicenters (black circles) are from the ANSS Comprehensive Catalog (see Data and Resources), and the 9 June 1981 epicenter is from Pennington and Carlson (1984). (b) Center earthquake magnitudes as a function of time and total monthly volumes for the injection well near the Center cluster. Note that seismicity is detected prior to injection at the well.

relationship between seismicity and oil and gas activities in this region, because it is possible these earthquakes are associated with ongoing natural seismicity in the area or are related to wastewater injection or a combination of both.

Other Earthquakes

We identified three earthquakes in southern Louisiana and Mississippi, of which one was identified by other agencies (see the Seismicity section). There are numerous wastewater injection wells across southern Louisiana (Weingarten *et al.*, 2015) in a zone with many growth faults extending out to the Gulf of Mexico. Reactivation of faults has likely occurred during hydrocarbon extraction and can result in surface subsidence (e.g., Chan and Zoback, 2007). There was one earthquake reported by the ANSS Comprehensive Catalog between 1980 and 2010 (black open circle in southern Louisiana in Fig. 1; see Data and Resources), in addition to historical earthquakes near Lake Charles in 1952 (Davis *et al.*, 1995) and in 1983 (Stevenson and Agnew, 1988). Also, earthquakes have occurred in southern Alabama and Mississippi (Gomberg and Wolf, 1999), with some relationship to hydrocarbon recovery efforts rather than wastewater injection. Nonetheless, the possibility of natural earthquakes cannot be ruled out. As we discuss in the Seismicity section, these earthquakes occurred when the TA was not yet installed in southeast Louisiana, and thus horizontal errors could be on the order of 10 s of kilometers. Because these individual events are not well located, we did not investigate them further and do not conclude whether they are induced or natural.

CONCLUSIONS

From an analysis of TA data, including application of a matched-filter technique, we identified about 40 previously unreported earthquakes in eastern Texas and Louisiana. We detected earthquakes in five distinct clusters; however, the majority of events were confined to zones near Timpson, Texas, and Bienville Parish, Louisiana. The Timpson sequence has been studied and discussed extensively by Frohlich *et al.* (2014). We identified a new cluster of seismicity in the Bienville Parish, Louisiana, which seems to exhibit swarm-like behavior. Because of the distance (~10 km) from active injectors and without further geomechanical information, we cannot directly link this activity to wastewater injection, though it is possible. The more likely scenario is that hydraulic fracturing induced the small-magnitude (M_L < 2.0) Bienville Parish seismic swarm; however, it is possible the events are natural. Near Center, Texas, we identify a cluster of seismicity that is within 5 km of an active injection well where maximum injection rates exceed 200, 000 bbl/month, though that seismicity appears to have begun prior to reported injection activities. This may be a case of a larger earthquake being triggered by injection in an area already experiencing seismicity. Previous to our study time period (Pennington and Carlson, 1984) and since our study (the Relation to Wastewater Injection and Hydraulic Fracturing section), there have been other events with a possible link to wastewater injection in the Center, Texas area (Fig. 5). This work highlights the complicated nature of investigating seismicity sequences and underlines the continued need for more comprehensive seismic networks monitoring.

Studies that suggest a potential link between human activity and seismicity should also consider whether natural tectonic events are possible. Because of the historical paucity of permanent seismic stations in the south-central United States, there is only limited information available about Louisiana's past seismicity over the last century (e.g., Stevenson and Agnew, 1988; Brasseaux and Lock, 1992; Ellsworth *et al.*, 2012). Without this historical context, it is difficult to determine whether earthquakes are natural or induced in regions of increasing energy production, especially those near sites of wastewater disposal or production operations. Prior to the TA, it is likely that humans would not have felt the seismicity in the Bienville Parish and Center/Border clusters; and, thus, it is possible that seismicity there is ongoing and natural. Nonetheless, the hydraulic fracturing in the area near Bienville Parish and

the increase in wastewater disposal near Center, Texas, followed by the occurrence of seismicity seems an unlikely coincidence. It therefore is possible that hydraulic fracturing induced previously undetected seismicity within the northwest portion of Louisiana and that wastewater injection may have induced seismicity in eastern Texas.

DATA AND RESOURCES

Past seismicity data included in the figures were obtained from the Advanced National Seismic System (ANSS) Comprehensive Catalog (http://earthquake.usgs.gov/earthquakes/search/, last accessed July 2015). Seismograms were downloaded from the Incorporated Research Institutions for Seismology (IRIS) Data Management Center, and those data were collected for the USArray Transportable Array (TA) experiment (doi: 10.7914/SN/TA). Some of the figures were created using Generic Mapping Tools (Wessel *et al.*, 2013). The detailed maps were obtained from the Texas Railroad Commission Public GIS Viewer (http://wwwgisp.rrc.state.tx.us/GISViewer2/, last accessed July 2015), the U.S. Geological Survey (USGS) Quaternary Faults and Folds Database (http://earthquakes.usgs.gov/regional/qfaults/, last accessed July 2015), the U.S. Energy Information Administration, obtained from http://www.eia.gov/pub/oil_gas/natural_gas/analysis_publications/maps/maps.htm (last accessed August 2015), and Geomap Company (2012).

ACKNOWLEDGMENTS

This research was partially supported by the U.S. Geological Survey (USGS), Department of the Interior under USGS Award Number G13AP00023 and by Research Partnership to Secure Energy for America Subcontract Number 11122-27. The views and conclusions contained in this document are those of the authors and should not be interpreted as representing the official policies, either expressed or implied, of the U.S. Government. We thank Rob Skoumal and two anonymous reviewers whose comments greatly improved this article.

REFERENCES

BC Oil and Gas Commission (2014). *Investigation of Observed Seismicity in the Montney Trend*, Victoria, British Columbia, Canada.

Brasseaux, C. A., and B. E. Lock (1992). The Opelousas earthquakes of 1823 and 1870, Louisiana history, *J. Louis. Hist. Assoc.* **33,** 317–324.

Chan, A. W., and M. D. Zoback (2007). The role of hydrocarbon production on land subsidence and fault reactivation in the Louisiana coastal zone, *J. Coast. Res.* **23,** no. 3, 771–786.

Davis, S. D., P. A. Nyffenegger, and C. Frohlich (1995). The 9 April 1993 earthquake in south-central Texas: Was it induced by fluid withdrawal? *Bull. Seismol. Soc. Am.* **85,** no. 6, 1888–1895.

Ellsworth, W. L., S. Horton, H. Benz, S. Hickman, A. Leeds, W. S. Leith, M. Meremonte, J. L. Rubinstein, M. M. Withers, and R. B. Herrman (2012). Tremors in the bayou: The events on the Napoleonville Salt Dome, Louisiana, *AGU Fall Meeting*, Abstract S51E-2453.

Ewing, T. E., and R. F. Lopez (1991). Principal structural features, Gulf of Mexico basin, in *The Geology of North America: The Gulf of Mexico Basin*, A. Salvador (Editor), Geological Society of America, Boulder, Colorado.

Friberg, P. A., G. M. Besana-Ostman, and I. Dricker (2014). Characterization of an earthquake sequence triggered by hydraulic fracturing in Harrison County, Ohio, *Seismol. Res. Lett.* **85,** no. 6, 1295–1307, doi: 10.1785/0220140127.

Frohlich, C., and S. D. Davis (2002). *Texas Earthquakes*, University of Texas Press, Austin, Texas, 275 pp.

Frohlich, C., W. Ellsworth, W. A. Brown, M. Brunt, J. H. Luetgert, T. MacDonald, and S. Walter (2014). The 17 May 2012 M 4.8 earthquake near Timpson, east Texas: An event possibly triggered by fluid injection, *J. Geophys. Res.* **119,** 581–593, doi: 10.1002/2013JB010755.

Frohlich, C., C. Hayward, B. W. Stump, and E. Potter (2011). The Dallas-Fort Worth earthquake sequence: October 2008 through May 2009, *Bull. Seismol. Soc. Am.* **101,** 327–340.

Frohlich, C., J. I. Walter, and J. F. W. Gale (2015). Analysis of Transportable Array (USArray) data shows earthquakes are scarce near injection wells in the Williston basin, 2008–2011, *Seismol. Res. Lett.* **86,** 492–499.

Geomap Company (2012). Executive reference map 302–east Texas (2012 Edition), map scale 1:380,160, https://www.geomap.com/georef.shtml (last accessed July 2015).

Gomberg, J., and L. Wolf (1999). Possible cause for an improbable earthquake: The 1997 M_w 4.9 southern Alabama earthquake and hydrocarbon recovery, *Geology* **27,** no. 4, 367–370.

Henley, A. D. (1965). *Seismic Activity Near the Texas Gulf Coast, National Convention*, Association of Engineering Geologists, Denver, Colorado.

Hornbach, M. J., H. R. DeShon, W. L. Ellsworth, B. W. Stump, C. Hayward, C. Frohlich, H. R. Oldham, J. E. Olson, M. B. Magnani, C. Brokaw, *et al.* (2015). Causal factors for seismicity near Azle, Texas, *Nat. Comm.* **6,** Article Number 6728, doi: 10.1038/ncomms7728.

Horton, S. (2012). Disposal of hydrofracking waste fluid by injection into subsurface aquifers triggers earthquake swarm in central Arkansas with potential for damaging earthquake, *Seismol. Res. Lett.* **83,** 250–260, doi: 10.1785/gssrl.83.2.250.

Hutton, L. K., and D. M. Boore (1987). The M_L scale in southern California, *Bull. Seismol. Soc. Am.* **77,** 2074–2094.

Kang, I. B., M. S. Jun, and J. S. Shin (2000). Research on local magnitude (M_L) scale in and near the Korean Peninsula, *Ann. Geophys.* **43,** no. 5, doi: 10.4401/ag-3674.

Kato, A., K. Obara, T. Igarashi, H. Tsuruoka, S. Nakagawa, and N. Hirata (2012). Propagation of slow slip leading up to the 2011 M_w 9.0 Tohoku-Oki earthquake, *Science* **335,** no. 6069, 705–708, doi: 10.1126/science.1215141.

Keranen, K., M. Weingarten, G. A. Abers, B. Bekins, and S. Ge (2014). Sharp increase in central Oklahoma seismicity since 2008 induced by massive wastewater injection, *Science* **345,** 448–451.

Kim, W.-Y. (1998). The M_L scale in eastern North America, *Bull. Seismol. Soc. Am.* **88,** 935–951.

Kim, W.-Y. (2013). Induced seismicity associated with fluid injection into a deep well in Youngstown, Ohio, *J. Geophys. Res.* **118,** no. 7, 3506–3518, doi: 10.1002/jgrb.50247.

McGarr, A. (2014). Maximum magnitude earthquakes induced by fluid injection, *J. Geophys. Res.* **119,** no. 2, 1008–1019, doi: 10.1002/2013JB010597.

Meng, X., Z. Peng, and J. L. Hardebeck (2013). Seismicity around Parkfield correlates with static shear stress changes following the 2003 M_w 6.5 San Simeon earthquake, *J. Geophys. Res.* **118,** 3576–3591, doi: 10.1002/jgrb.50271.

Meng, X., X. Yu, Z. Peng, and B. Hong (2012). Detecting earthquakes around Salton Sea following the 2010 M_w 7.2 El Mayor-Cucapah earthquake using GPU parallel computing, *Procedia Comput. Sci.* **9,** 937–946, doi: 10.1016/j.procs.2012.04.100.

Pavlis, G., F. Vernon, D. Harvey, and D. Quinlan (2004). The generalized earthquake-location (GENLOC) package: An earthquake location library, *Comput. Geosci.* **30,** 1079–1091.

Peng, Z., and P. Zhao (2009). Migration of early aftershocks following the 2004 Parkfield earthquake, *Nat. Geosci.* **2,** 877–881, doi: 10.1038/ngeo697.

Pennington, W. D., and S. M. Carlson (1984). Observations from the East Texas Seismic Network (June 1981–August 1982), *Univ. Texas Bureau Econ. Geol. Circular* **84,** no. 3, 48.

Richter, C. F. (1935). An instrumental earthquake magnitude scale, *Bull. Seismol. Soc. Am.* **25,** 1–32.

Richter, C. F. (1958). *Elementary Seismology*, W. H. Freeman and Company, San Francisco, California, 768 pp.

Rubinstein, J. L., and A. B. Mahani (2015). Myths and facts on wastewater injection, hydraulic fracturing, enhanced oil recovery, and induced seismicity, *Seismol. Res. Lett.* **84,** doi: 10.1785/0220150067.

Rubinstein, J. L., W. L. Ellsworth, A. McGarr, and J. Benz (2014). The 2001-present induced earthquake sequence in the Raton basin of northern New Mexico and southern Colorado, *Bull. Seismol. Soc. Am.* **104,** no. 5, 2162–2181.

Schaff, D. P., and P. G. Richards (2014). Improvements in magnitude precision, using the statistics of relative amplitudes measured by cross correlation, *Geophys. J. Int.* **197,** no. 1, 335–350, doi: 10.1093/gji/ggt433.

Shearer, P. M. (1994). Global seismic event detection using a matched filter on long-period seismograms, *J. Geophys. Res.* **99,** no. B7, 13,713–13,725.

Shelly, D. R., G. C. Beroza, and S. Ide (2007). Non-volcanic tremor and low frequency earthquake swarms, *Nature* **446,** 305–307, doi: 10.1038/nature05666.

Skoumal, R. J., M. R. Brudzinski, and B. S. Currie (2015). Earthquakes induced by hydraulic fracturing in Poland Township, Ohio, *Bull. Seismol. Soc. Am.* **105,** no. 1, 189–197, doi: 10.1785/0120140168.

Skoumal, R. J., M. R. Brudzinski, B. S. Currie, and J. Levy (2014). Optimizing multi-station earthquake template matching through re-examination of the Youngstown, Ohio sequence, *Earth Planet. Sci. Lett.* **405,** 274–280.

Stevenson, D. A., and J. D. Agnew (1988). Lake Charles, Louisiana, earthquake of 16 October 1983, *Bull. Seismol. Soc. Am.* **78,** 1463–1474.

Stevenson, D. A., and R. P. McCulloh (2001). Earthquakes in Louisiana, *Louisiana Geol. Surv. Public Information Series No. 7*, 8 pp.

Waldhauser, F., and W. L. Ellsworth (2000). A double-difference earthquake location algorithm: Method and application to the northern Hayward fault, *Bull. Seismol. Soc. Am.* **90,** 1353–1368.

Walter, J. I., Z. Peng, X. Meng, A. V. Newman, S. Y. Schwartz, and M. Protti (2015). Far-field triggering of foreshocks near the nucleation zone of the 5 September 2012 (M_w 7.6) Nicoya Peninsula, Costa Rica earthquake, *Earth Planet. Sci. Lett.* **431,** 75–86, doi: 10.1016/j.epsl.2015.09.017.

Weingarten, M., S. Ge, J. W. Godt, B. A. Bekins, and J. L. Rubinstein (2015). High-rate injection is associated with the increase in US mid-continent seismicity, *Science* **348,** no. 6241, 1336–1340.

Wessel, P., W. H. F. Smith, R. Scharroo, J. Luis, and F. Wobbe (2013). Generic mapping tools: Improved version released, *Eos Trans. AGU* **94,** no. 45, 409–410.

Jacob I. Walter
Peter J. Dotray
Cliff Frohlich
Institute for Geophysics
University of Texas at Austin
10100 Burnet Road (R2200)
Austin, Texas 78758-4445 U.S.A.
jwalter@ig.utexas.edu

Julia F. W. Gale
Bureau of Economic Geology
University of Texas at Austin
Austin, Texas 78758-4445 U.S.A.

Published Online 10 February 2016
Corrected Online 17 February 2016